Chinese Chemical Letters 33 (2022) 4617–4622

Contents lists available at ScienceDirect

Chinese Chemical Letters

journal homepage: www.elsevier.com/locate/cclet

Oral delivery of superoxide dismutase by lipid polymer hybrid nanoparticles for the treatment of ulcerative colitis

Yaxin Cui, Tianyu Zhu, Xueyan Zhang, Jicong Chen, Fengying Sun, Youxin Li*, Lesheng Teng*

School of Life Sciences, Jilin University, Changchun 130012, China

ARTICLE INFO

Article history:
Received 11 November 2021
Revised 12 March 2022
Accepted 16 March 2022
Available online 19 March 2022

Keywords:
Superoxide dismutase
PCADK DSPE-PEG
Cell-penetrating peptide
Ulcerative colitis
Lipid polymer hybrid nanoparticles

ABSTRACT

Protein-based drugs have received extensive attention in the field of drug research in recent years. However, protein-based drug activity is difficult to maintain during oral delivery, which limits its application. This study developed bifunctional oral lipid polymer hybrid nanoparticles (R8-PEG-PPNPs) that deliver superoxide dismutase (SOD) for the treatment of ulcerative colitis (UC). R8-PEG-PPNPs was composed of PCADK, PLGA, lecithin, and co-modified with stearic acid-octa-arginine and polyethylene glycol. The nanoparticles (NPs) are uniformly dispersed with a complete spherical structure. *In vitro* stability and release studies showed that R8-PEG-PPNPs exhibited good stability and protection. *In vitro* cell culture experiments demonstrated that R8-PEG-PPNPs as carriers have no significant toxic effects on cells at concentration below 1000 μg/mL and promote cellular uptake. In experiments with ulcerative colitis mice, R8-PEG- PPNPs were able to enhance drug absorption by intestinal epithelial cells and accumulate effectively at the site of inflammation. Its therapeutic effect further demonstrates that R8-PEG-PPNPs are a promising delivery system for oral delivery of protein-based drugs.

Protein-based drugs have the advantages of high biological activity, good specificity and significant therapeutic effects, and have received wide attention in the treatment of various diseases in recent years [1]. After oral absorption, protein drugs are absorbed into the blood circulation through the gastrointestinal tract and can achieve local and systemic treatment [2]. However, the application of protein drugs is greatly limited by their high hydrophilicity, susceptibility to destruction by proteases and extreme pH, and difficulty in penetrating through intestinal epithelial cells by passive diffusion [3–6]. Therefore, nanodrug delivery systems including liposomes, micelles, and polymeric nanoparticles have been developed as potential carriers for the delivery of protein drugs [7–11]. Lipid polymer hybrid nanoparticles (LPNPs) are new drug delivery systems developed by combining the advantages of liposomes and polymer nanoparticles, which are characterized by small particle size, good drug encapsulation ability and good biocompatibility [12,13].

The delivery strategy of protein drugs is different from that of traditional drugs [14]. Since protein drugs do not easily penetrate intestinal epithelial cells and mucus layer, we prefer that the NPs are transported by intestinal epithelial cells and interact with inflammatory cells in the submucosa [15–17]. NPs trapped in the gut can also release drugs to treat colitis. However, NPs encounter mucus and intestinal epithelial cell barriers during oral delivery [18–20]. In order to overcome the mucus barrier, we believe that hydrophilic particles with small particle size and uncharged or overall electrically neutral surfaces (*e.g.*, PEGylation) are more likely to pass through the mucus layer [21–24]. However, this mucus inert surface reduces the affinity with the cell membrane that is lipophilic and negatively charged, thus reducing the cellular uptake efficiency [25,26]. Cell-penetrating peptides (*e.g.*, hydrophobic derivatives of octa-arginine with stearic acids, Sta-R8) can improve the cell penetration of drugs and drug carriers [27,28]. It is currently widely studied and used in drug delivery systems [29]. pH-responsive drug delivery systems have been extensively investigated in inflammatory therapies. PCADK is a novel Polyketide with improved acid-sensitive hydrolysis properties [30–32].

Therefore, we synthesized LPNPs with Sta-R8, PEG, PCADK, PLGA and lipids. Lipids provide protection in the outer layer of the NPs and increase biocompatibility. PCADK enables the timely release of protein drugs from NPs within the acidic environment of inflammatory cells. PEG modification increases the hydrophilicity of the NPs surface and facilitates the passage through the mucus layer. Sta-R8 improves the absorption efficiency of small intestinal epithelial cells. Co-modification of positively charged Sta-R8 and

* Corresponding authors.
E-mail addresses: liyouxin@jlu.edu.cn (Y. Li), tenglesheng@jlu.edu.cn (L. Teng).

https://doi.org/10.1016/j.cclet.2022.03.077
1001-8417/

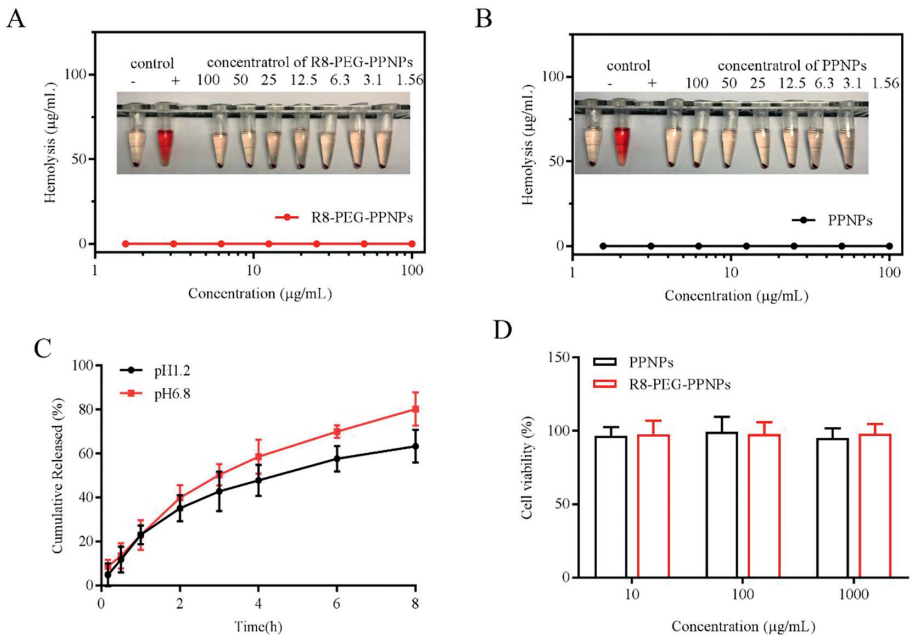

Fig. 1. Hemolysis of (A) PPNPs and (B) R8-PEG-PPNPs. (C) *In vitro* release curve of R8-PEG-PPNPs at 37 °C. Values are mean ± SD ($n = 3$). (D) The cytotoxicity of nanoparticle carriers on activated RAW 264.7. Values are mean ± SD ($n = 6$).

negatively charged PEG yields near-electrically neutral LPNPs. Finally, the anti-inflammatory effect of orally administered SOD LPNPs was investigated in mice with ulcerative colitis.

For individual barriers during oral absorption, we have developed a nano-delivery system that effectively delivers SOD to treat UC. In the current study, R8 improves the efficiency of NPs entry into cells. PCADK is a pH-responsive material. The PEGylation modification of the NPs itself and the expression of the NPs are close to electrical neutrality, which effectively improves the penetration of the mucus layer. Here, the inner carrier of LPNPs is composed of PCADK and PLGA. The lipid layer protects the exterior of the NPs and improves biocompatibility. During the preparation process, we adjust the composition ratio in order to obtain NPs with smaller particle size and relatively large drug loading. As shown in Table S1 (Supporting information), with the increase of lipids (from the first batch to the fifth batch), the particle size and the drug loading volume gradually decreased. We choose batch 4 drug loading volume gradually decreased. We choose batch with smaller particle size and a relatively high drug load. With the decrease of PLGA:PCADK from 10:0 to 4:6, the particle size of the NPs first increased and then decreased, but the drug loading of the NPs gradually decreased. Batch 6 has a relatively high drug load. Finally, we replaced part of the lipid with R8 and added DSPE-PEG. Taking into account the electrical factors, batch 16 (R8-PEG-PPNPs) close to electrically neutral NPs was selected for further research. Batch 6 (PPNPs) served as a control group.

The average particle size of R8-PEG-PPNPs detected by a nanoparticle size analyzer is 136.0 ± 1.17 nm. It can be seen from the distribution diagram (Fig. S1 in Supporting information) that it has a single particle size peak. The structure of R8-PEG-PPNPs obtained by scanning electron microscopy is shown in Fig. S2 (Supporting information), and the NPs appear as nearly spherical structures. The average particle size of R8-PEG-PPNPs detected by SEM is not much different from the DLS result.

NPs were dispersed in different media, and the particle size and PDI of LPNPs were measured for 7 days at 4 °C and 37 °C. Fig. S3 (Supporting information) are the changes in particle size and PDI at 4 °C. The particle size and PDI did not change significantly within 4 days. These data support that the NPs can be stored at 4 °C for future use. Fig. S4 (Supporting information) are the experimental results at 37 °C. There was no significant change in particle size and PDI, which indicates that NPs can exist stably at 37 °C. Since LPNPs can be quickly and evenly distributed after entering the blood circulatory system, LPNPs can stably exist in the body.

Then, we investigated their stability in the presence of enzymes (pepsin or trypsin) in simulated gastric fluid (SGF, pH 2.0) and simulated intestinal fluid (SIF, pH 6.8), respectively. As shown in Fig. S5 (Supporting information), the NPs all exhibited excellent particle stability in SGF (incubation for 2 h) or SIF (incubation for 6 h) containing pepsin or trypsin, with no significant variation of size. The above results confirmed that NPs could keep its particle structure stable in both *in vivo* (SGF and SIF) environments.

In order to study the biocompatibility of NPs, we conducted a hemolysis experiment of NPs. After incubating R8-PEG-PPNPs/PPNPs with different concentrations (1.56-100.0 μg/mL) with red blood cells, the red blood cells did not rupture and the hemolysis rate was less than 3% (Figs. 1A and B). This result shows that R8-PEG-PPNPs and PPNPs will not cause hemolysis of red blood cells and have good biocompatibility. To evaluate the drug release from R8-PEG-PPNPs in gastric and intestinal fluid environments, the SOD release behavior of R8-PEG-PPNPs in two release media SGF (pH 1.2) and SIF (pH 6.8) was investigated. As shown in Fig. 1C, R8-PEG-PPNPs exhibited a biphasic release pattern in both release media. The faster drug release in the first hour may be caused by the rapid diffusion of the unencapsulated drug and the sudden release of the NPs. The slow release of the drug afterward is due to the fact that the NPs are releasing the drug slowly.

Meanwhile, we also observed that the release rate of R8-PEG-PPNPs was significantly higher in SIF (pH 6.8) than in SGF (pH 1.2). It may be due to the fact that the critical micelle concentration of the excipients of NPs (*e.g.*, ePC) decreases with decreasing pH, making the structure more stable reducing the rate of drug release. These results suggest that the release of LPNPs has a protective effect.

MTT assay to assess the cytotoxicity of nanoparticle carriers on activated RAW 264.7. Fig. 1D shows the results of the effect of different concentrations of nanoparticle carriers on cells. The cell sur-

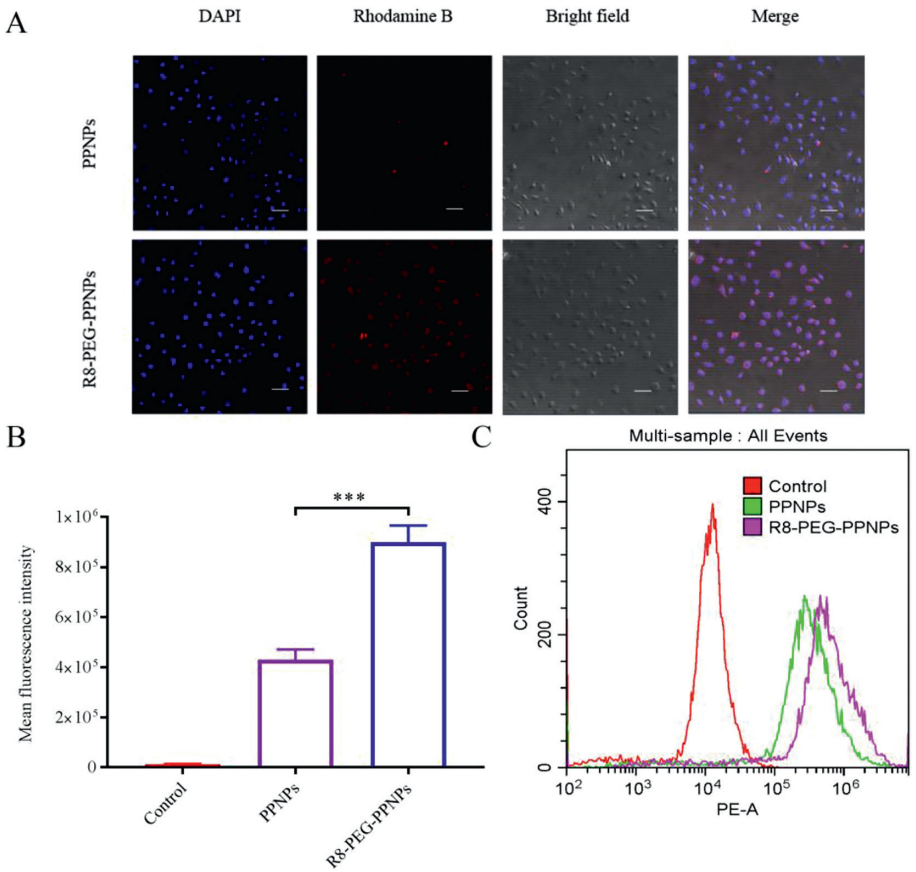

Fig. 2. (A) Intracellular distribution of NPs in RAW 264.7 cells by CLSM (200×; scale bar: 50 μm). (B) Representative flow cytometric curves. Values are mean ± SD ($n = 3$, $^{***}P < 0.001$). (C) Quantitative data of flow cytometric.

vival rates were above 95%, indicating that both nanoparticle carriers would not be cytotoxic to RAW 264.7.

In the inflammatory cell model constructed from activated RAW 264.7, rhodamine B was encapsulated by NPs in order to visualize the intracellular distribution of NPs. As shown in Fig. 2A, rhodamine B is the red fluorescence that can be observed around the nucleus of the cell. The red fluorescence of the R8-PEG-PPNPs group was stronger than that of the PPNPs group which indicated that R8 and PEG together promoted the uptake of NPs by activated RAW 264.7.

And later, further quantitative analysis was performed by flow cytometry (EPICS XL). The results showed that the Control group had the lowest intracellular fluorescence intensity (Figs. 2B and C). Phase uptake was significantly higher in the R8-PEG-PPNPs group compared with the other groups ($P < 0.001$). This is consistent with the CLSM observations and validates that R8 and PEG promote the uptake of inflammatory cells.

Before examining the efficacy of NPs *in vivo*, we studied the distribution of NPs constructed by Dir *in vivo* tissues. All animal care and experiments are carried out in accordance with the guidelines for the humane treatment of experimental animals in Jilin University (Nos. SY202012023 and SY202105016). Ulcerative colitis model is a common inflammatory bowel disease induced by oral administration of 3% dextran sodium sulfate (DSS) aqueous solution for 7 days. Twelve hours after oral administration of the drug, we observed the fluorescence distribution in mice (Fig. 3A). The weaker fluorescence intensity of the Dir group indicates that Dir is difficult to be digested and absorbed into the body. In contrast, the R8-PEG-PPNPs group showed stronger fluorescence intensity at the site of inflammation than the other groups. Some studies indicate that the NPs lodge in intestinal tract and release drugs that can treat the colon [33–35]. As the above experimental results show, most of our NPs are concentrated in the colon.

Subsequently, we investigated the *in vivo* anti-inflammatory efficacy of NPs in mice with ulcerative colitis. Mice in the model group showed a significant increase in body mass index and disease activity index (DAI) during the 7 days of DSS induction (Figs. 3B and C). In this case, the anti-inflammatory effect of the SOD group was not significantly different from that of the model group. In contrast, the PPNPs group only slightly alleviated the weight loss. In comparison, the R8-PEG-PPNPs group showed a significant reduction in DAI index and significant alleviation of weight loss. Consistent with these results, examination of colonic length after mice were euthanized (Fig. 3D). Compared to the control group, the colonic length of mice in the model group was significantly shorter ($P < 0.001$). Compared with the model group, the colon length of mice in the SOD group increased only by 4.69%, that of mice in the PPNPs group increased by 18.11%, and that of mice in the R8-PEG-PPNPs group increased significantly by 32.32% ($P < 0.01$). These data further demonstrate that R8-PEG-PPNPs significantly inhibit colonic shortening in UC mice.

In addition, we recorded the spleen weight of UC mice as a macroscopic feature to analyze the severity of colitis (Fig. 3E). Splenomegaly is considered to be an important indicator of the degree of inflammation in colitis [36]. Mice in the model group had a highly significant increase in spleen coefficient compared to the blank group ($P < 0.01$), which indicates severe colitis inflammation. The splenic index of the free SOD group was almost comparable to that of the control group and showed no alleviating effect. In comparison, the splenic coefficient was significantly lower in the remaining two groups. Notably, there was a significant reduction in

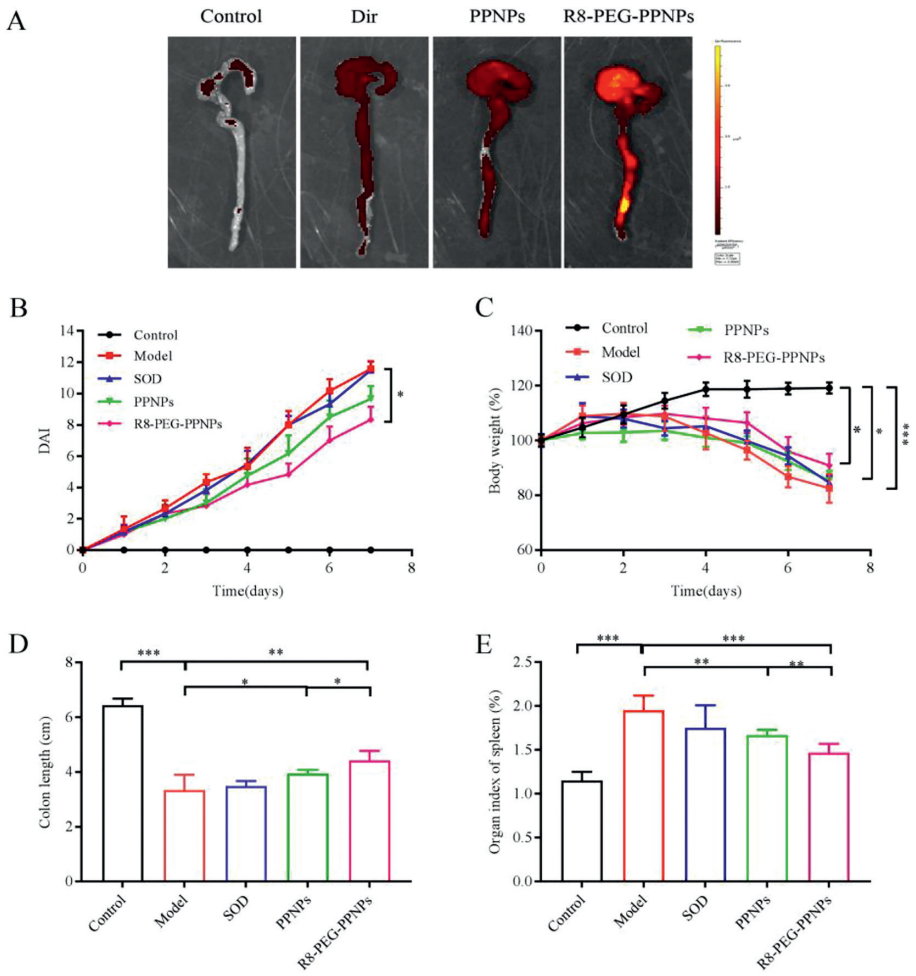

Fig. 3. (A) *Ex vivo* images illustrating NPs distribution in the mice with DSS colitis. (B) Macroscopical evaluation of the therapeutic effect of NPs on DSS-induced ulcerative colitis in mice ($n = 6$). (C) Changes in DAI of ulcerative colitis mice. Changes in body weight of mice during 7 days of treatment ($n = 6$, Data were normalized as a percentage of the bodyweight at day 1). (D) The length of colonic tissues isolated from ulcerative colitis mice at day 7 ($n = 5$). (E) The spleen index was examined after the mice were euthanized at day 7 ($n = 6$). Data are mean ± SD. $^{*}P < 0.05$, $^{**}P < 0.01$, $^{***}P < 0.001$.

the splenic coefficient in the R8-PEG-PPNPs group compared with the PPNPs group ($P < 0.01$). The above data suggest that R8-PEG-PPNPs are more effective than PPNPs in improving macroscopic changes in ulcerative colitis.

After the mice were euthanized, we performed a pathological analysis of the colonic tissues of the mice in the different treatment groups (Fig. 4A). The negative control sections had clearly visible cup cells and minimal inflammatory cell infiltration. In contrast, colon sections from untreated mice with ulcerative colitis showed intestinal epithelial necrosis, lamina propria hyperplasia, loss of cupped cells, and a large infiltration of inflammatory cells. Compared to other treatment groups, R8-PEG-PPNPs administration was better at reducing inflammatory cell infiltration and effectively preventing mucosal epithelial cell necrosis and lamina propria proliferation. The results further suggest that R8-PEG-PPNPs have a palliative effect on ulcerative colitis in mice. Mice treated with SOD did not significantly improve the histological features of colitis.

Low inflammatory cell infiltration in the plasma of mice in the R8-PEG-PPNPs treatment group was further confirmed by measuring the plasma levels of IL-1β and IL-6 in mice (Figs. 4B and C). The levels of IL-1β and IL-6 in model mice increased significantly with the induction of colitis compared to normal mice. Meanwhile, oral administration of SOD did not significantly reduce the levels of IL-1β and IL-6 in UC mice. In contrast, the intervention of PPNPs and R8-PEG-PPNPs resulted in a significant decrease in IL-1β and IL-6 levels. Notably, R8-PEG-PPNPs exhibited better anti-inflammatory effects compared with PPNPs. These results suggest that Sta-R8 and PEG-modified LPNPs can better deliver SOD, improve drug uptake efficiency, and achieve better therapeutic effects.

We initially evaluated whether this therapy produced side effects on the organs of mice with ulcerative colitis by studying H&E-stained pathological sections of the liver, spleen and kidneys. No significant abnormalities such as cellular edema, inflammatory cell infiltration, congestion or vascular microstructural changes were found in the treatment group (Fig. 4D). These findings confirm that this assay exhibits a good safety profile for oral administration.

In this study, Sta-R8 and DSPE-PEG co-modified PCADK/PLGA oral LPNPs were developed for the treatment of ulcerative colitis. The optimized NPs were obtained with a particle size of 136.0 ± 1.17 nm, narrow size distribution (PDI of 0.182 ± 0.028), and near-neutral potential (2.8 ± 0.26 mV). *In vitro* stability and release behavior study, R8-PEG-PPNPs showed good stability and protection. In cytological level studies, nanoparticle carriers had no toxic effects on cells and R8-PEG-PPNPs were able to improve drug uptake efficiency. The results of experiments in mice with ulcerative colitis showed that R8-PEG-PPNPs exhibited good anti-inflammatory effects. Meanwhile, the nano-delivery system exhibited a good safety profile. In conclusion, our results suggest that

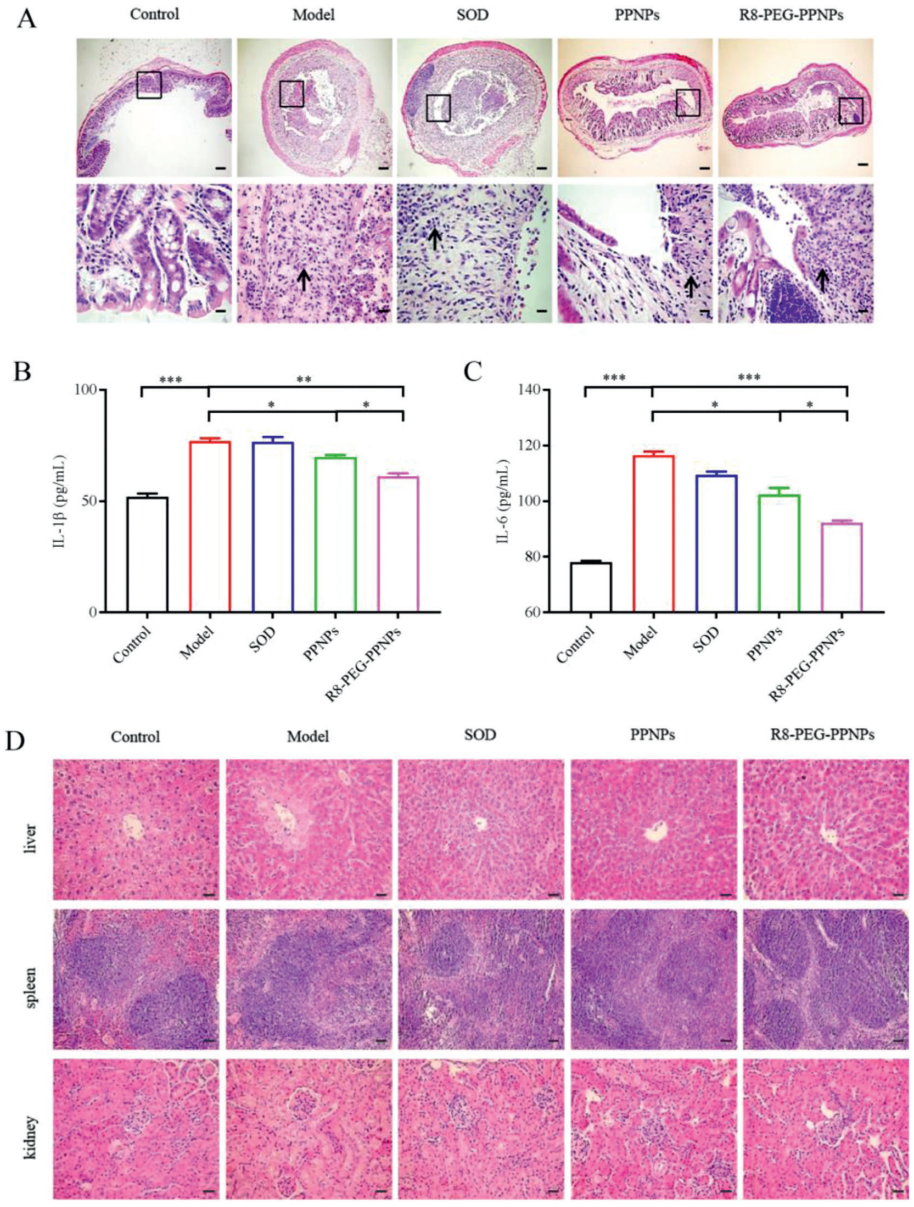

Fig. 4. (A) H&E-stained pathological sections of colonic tissues from different groups. (40×, 400×; Scale bars: 200, 20 μm). Expression levels of IL-1β (B) and IL-6 (C) in mouse plasma. Values are mean ± SD ($n = 6$, $^{*}P < 0.05$, $^{**}P < 0.01$, $^{***}P < 0.001$). (D) H&E sections of the liver, spleen and kidney in ulcerative colitis mice (200×; Scale bar: 50 μm).

R8-PEG-PPNPs have great potential for oral delivery of SOD for the treatment of ulcerative colitis.

Declaration of competing interest

The authors declare no conflict of interest.

Acknowledgments

The authors acknowledge the financial support received form National Natural Science Foundation of China (No. 82073784), Jilin Province Science and Technology Development Program (No. 20200801012GH) and Industrial Technology Research and Development Projects from the Development and Reform Commission of Jilin Province (No. 2019C050-4). Meanwhile, the authors also acknowledge Key Laboratory of Pathobiology, Ministry of Education, Jilin University.

Supplementary materials

Supplementary material associated with this article can be found, in the online version, at doi:10.1016/j.cclet.2022.03.077.

References

[1] S. Khafagy el, M. Morishita, Y. Onuki, K. Takayama, Adv. Drug Deliv. Rev. 59 (2007) 1521–1546.
[2] L.M. Ensign, R. Cone, J. Hanes, Adv. Drug Deliv. Rev. 64 (2012) 557–570.
[3] A.A. Date, J. Hanes, L.M. Ensign, J. Control. Release 240 (2016) 504–526.
[4] N. Marasini, M. Skwarczynski, I. Toth, Expert Rev. Vaccines 13 (2014) 1361–1376.
[5] J. Sheng, H. He, L. Han, et al., J. Control. Release 233 (2016) 181–190.
[6] M. Yang, S.K. Lai, Y.Y. Wang, et al., Angew. Chem. Int. Ed. 50 (2011) 2597–2600.
[7] S.S. Lucky, N.M. Idris, K. Huang, et al., Theranostics 6 (2016) 1844–1865.
[8] J. Xie, J. Huang, X. Li, S. Sun, X. Chen, Curr. Med. Chem. 16 (2009) 1278–1294.
[9] J. Xie, G. Liu, H.S. Eden, H. Ai, X. Chen, Acc. Chem. Res. 44 (2011) 883–892.
[10] H.B. Ruttala, N. Chitrapriya, K. Kaliraj, et al., Acta Biomater. 63 (2017) 135–149.
[11] H.T. Shi, X.Y. Zhao, J.S. Gao, et al., Chin. Chem. Lett. 31 (2020) 3102–3106.
[12] L. Zhang, J.M. Chan, F.X. Gu, et al., ACS Nano 2 (2008) 1696–1702.
[13] S.N. Zhao, J.H. Li, F.Z. Wang, et al., Chin. Chem. Lett. 31 (2020) 1147–1152.

[14] M. Zhang, D. Merlin, Inflamm. Bowel Dis. 24 (2018) 1401–1415.
[15] A.T. Florence, J. Drug Target. 12 (2004) 65–70.
[16] B. Xiao, Z. Zhang, E. Viennois, et al., Theranostics 6 (2016) 2250–2266.
[17] X. Pu, N. Ye, M. Lin, et al., Carbohyd. Polym. 273 (2021) 118612.
[18] W. Shan, X. Zhu, M. Liu, et al., ACS Nano 9 (2015) 2345–2356.
[19] M. Liu, J. Zhang, X. Zhu, et al., J. Control. Release 222 (2016) 67–77.
[20] X. Zhu, J. Wu, W. Shan, et al., Adv. Funct. Mater. 26 (2016) 2728–2738.
[21] C. He, Y. Hu, L. Yin, C. Tang, C. Yin, Biomaterials 31 (2010) 3657–3666.
[22] X. Murgia, P. Pawelzyk, U.F. Schaefer, et al., Biomacromolecules 17 (2016) 1536–1542.
[23] K. Maisel, L. Ensign, M. Reddy, R. Cone, J. Hanes, J. Control. Release 197 (2015) 48–57.
[24] J. Sheng, L. Han, J. Qin, et al., ACS Appl. Mater. Inter. 7 (2015) 15430–15441.
[25] A. Verma, F. Stellacci, Small 6 (2010) 12–21.
[26] E. Oh, J.B. Delehanty, K.E. Sapsford, et al., ACS Nano 5 (2011) 6434–6448.
[27] E. Böhmová, D. Machová, M. Pechar, et al., Physiol. Res. 67 (2018) S267–S279.
[28] Y. Chen, L. Yuan, L. Zhou, et al., Int. J. Nanomed. 7 (2012) 4581–4591.
[29] A. Falanga, L. Lombardi, E. Galdiero, V.D. Genio, S. Galdiero, Future Med. Chem. 12 (2020) 1431–1446.
[30] S.C. Yang, M. Bhide, I.N. Crispe, R.H. Pierce, N. Murthy, Bioconjug. Chem. 19 (2008) 1164–1169.
[31] F. Danhier, E. Ansorena, J.M. Silva, et al., J. Control. Release 161 (2012) 505–522.
[32] G. Hartmann, C. Bidlingmaier, B. Siegmund, et al., J. Pharmacol. Exp. Ther. 292 (2000) 22–30.
[33] H. Zhou, Y. Ikeuchi-Takahashi, Y. Hattori, H. Onishi, Int. J. Mol. Sci. 21 (2020) 2376.
[34] D. Wang, M. Sun, Y. Zhang, et al., Phytomedicine 78 (2020) 153293.
[35] J. Xu, M. Tam, S. Samaei, et al., Acta Biomater. 48 (2017) 247–257.
[36] M. Naeem, M.A. Oshi, J. Kim, et al., Nanomedicine 14 (2018) 823–834.